ON THE LEVEL OF APPROXIMATION OF THE MULTI-DIMENSIONAL POTENTIAL FLOW SOLUTION IN COMPLEX GEOMETRIES WITH THERMAL-HYDRAULIC SYSTEM CODES

C. Frepoli*, J. P. Yurko and J. W. Fricano
FPoliSolutions, LLC, 4618 Old William Penn Hwy, Murrysville, PA 15668, USA
*frepolc@fpolisolutions.com

F. Buschman and D. Aumiller
Bettis Atomic Power Laboratory, West Mifflin, PA 15122

ABSTRACT

This paper is among a series presented in this conference that illustrates the use of rather simple but fundamental canonical problems to challenge key aspects of the multidimensional flow process for the thermal-hydraulic code RELAP5-3D.

First of all, contrary to Computational Fluid Dynamics (CFD) codes, thermal-hydraulic codes are designed to approximate multi-dimensional flow to the level required for the specific engineering application. For instance the effect of viscosity is not explicitly modeled, but its effect is included in constitutive empirical relationships which were primarily derived from one-dimensional tests. Flow regime maps, also derived from one-dimensional steady-state datasets, are used to derive the constitutive relationships that apply to the different regimes.

Acknowledging these limitations, metrics for assessment can be established to ensure that a minimum set of requirements is met by the analytical tool, similar to those discussed in the other papers of this series.

The multidimensional capability of RELAP5-3D in single-phase flow is assessed by comparing the 2D or 3D solution obtained from the code to potential flow analytical solutions. Several of which are available in the literature for moderately complex geometries.

Solutions to the potential flow for a few selected geometries have been obtained and are compared with the prediction of RELAP5-3D. The geometries considered here can be encountered in the assessment of T/H codes (i.e., UPTF or others from the 2D/3D program). The potential flow problem is included into an automated verification suite which is described in another work submitted to this conference.

KEYWORDS:
Potential Flow, RELAP5-3D, Reactor Vessel Thermal-Hydraulics

1. INTRODUCTION

This paper is among a series presented in this conference that illustrates the use of fundamental canonical problems to challenge key aspects of the multidimensional flow solution process for the thermal-hydraulic system code RELAP5-3D [1] [2].

Thermal-hydraulic system codes are designed to approximate multi-dimensional flow to the level required for the specific engineering application of the code. Therefore, it is important for the analyst to be aware of these limitations and to understand their impact on the fidelity of the resulting solution. This judgment is also complicated by the reality that multi-dimensional multi-phase flow data is sparse and often does not allow a complete investigation of the code capabilities as part of the assessment process. However, expectations, or metrics, for the assessment can be established to ensure that a minimum set of requirements are met by the tool, justifying further investigation into its applicability.

In thermal-hydraulic system codes, the fluid viscosity is not explicitly modeled but its effect is included in constitutive empirical relationships, which are primarily derived from one-dimensional tests. Flow regimes maps, also derived from one-dimensional steady-state datasets are used to determine the constitutive relationships that are applied to the different regimes.

The RELAP5-3D multidimensional component features solutions of the 3D momentum equation for both inviscid and viscous laminar flow in Cartesian and cylindrical coordinates. An option exists to explicitly model laminar viscous stress terms for a realistic representation of multi-dimensional flow in both single phase and two-phase regimes [3].

A 3D domain can be connected to 1D components to allow modeling complex hydraulic systems. Internal walls in the multi-dimensional component can be used to simulate hardware that blocks flow paths within the flow domain. The RELAP5-3D manual recognizes some of the limitations in the model and provides appropriate workarounds for those discussed. The reader is encouraged to refer to Section 3.1.11 of [3] for more details. However a few key questions remain unanswered and the purpose of this paper is to investigate these issues.

One natural question is to investigate if RELAP5-3D is able to approximate inviscid, irrotational flow when viscosity effects are ignored in the model. A good benchmark to assess the multidimensional capability in single-phase flow is to compare the 2D or 3D solution obtained from the code to the potential flow analytical solutions which are available in the literature for some complex geometries.

The potential flow solutions of a few selected geometries have been obtained and are compared with predictions from RELAP5-3D. The multi-dimensional geometries considered are simple variations on geometries that are often encountered in the assessment matrices of evaluation models employing the code (i.e., UPTF or others from the 2D/3D program [4]).

The first fundamental problem selected for analysis is the classic backward facing step (also referred to as a channel with a sudden area expansion). The second problem approximates the flow from the downcomer into the lower plenum and up into the core of a typical Pressurized Water Reactor (PWR). Both are represented as 2D problems in Cartesian coordinates.

The backward facing step is a classic CFD problem used to analyze boundary layer separation around a sharp corner. Potential flow theory only holds for irrotational flow and is therefore not suited to capture such real phenomena. However, the goal here is not to validate the RELAP5-3D prediction against reality, but to gain insight into how the discretization approximations influence the RELAP5-3D multidimensional component. Therefore, the backward facing step in the present context is a *verification* problem that isolates the influence of numerical diffusion on a two-dimensional velocity field.

2. GOVERNING EQUATIONS

Assuming a 2D isothermal, incompressible liquid and an inviscid flow, the RELAP5-3D multi-dimensional governing equations reduce to the form:

$$\frac{\partial v_x}{\partial x} + \frac{\partial v_y}{\partial y} = 0 \tag{1}$$

$$\begin{aligned} \left(\frac{\partial v_x}{\partial t} + v_x \frac{\partial v_x}{\partial x} + v_y \frac{\partial v_x}{\partial y} \right) &= -\frac{1}{\rho}\frac{\partial P}{\partial x} + g_x \\ \left(\frac{\partial v_y}{\partial t} + v_x \frac{\partial v_y}{\partial x} + v_y \frac{\partial v_y}{\partial y} \right) &= -\frac{1}{\rho}\frac{\partial P}{\partial y} + g_y \end{aligned} \tag{2}$$

Equation (1) is the 2D incompressible continuity equation and Eq. (2) presents the 2D inviscid momentum equations.

3. POTENTIAL FLOW THEORY

Incompressible, irrotational, inviscid flow can be solved with potential flow theory which assumes the velocity is a gradient of a scalar function, the (velocity) potential:

$$\vec{u} = \nabla \varphi \tag{3}$$

Substitution of Eq. (3) into Eq. (1), yields the Laplace equation in 2D:

$$\nabla^2 \varphi = 0 = \frac{\partial^2 \varphi}{\partial x^2} + \frac{\partial^2 \varphi}{\partial y^2} \tag{4}$$

Rather than having to solve three equations for three unknowns (the velocity components and the pressure), potential flow theory reduced the problem to solving one equation with one unknown: the potential. This simplification is the main reason why potential flow theory has been employed to model inviscid flows [5].

The objective is to compare the RELAP5-3D solution to analytical solutions obtained from potential flow theory when the RELAP5-3D model is setup to model an incompressible, inviscid flow. Potential flow solutions in complex 2D and 3D geometries are presented by Yeh [6]. As described earlier, the first problem analyzed is the classic benchmark problem, the backward facing step. The problem domain is illustrated in Figure 1.

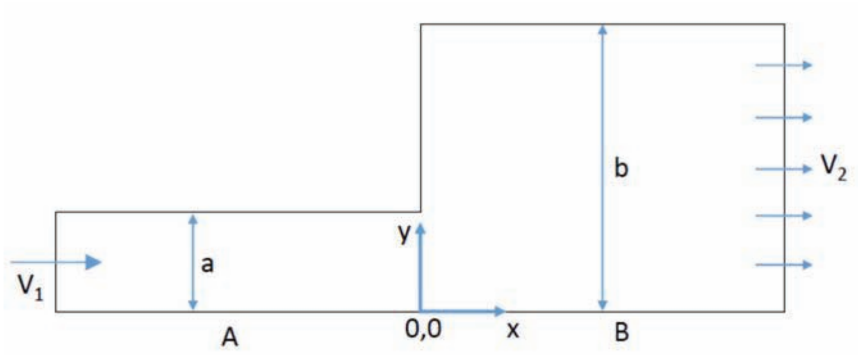

Figure 1 – Backward Facing Step

The analytical solution derivation is discussed in Appendix A. The solution is represented by the infinite series in Eq. (5) and Eq. (6) for the two regions shown in Figure 1. The velocity vector plots for the analytical solution computed at RELAP5-3D model cell centers are shown in Figure 2[1]. Note that the velocity field is adequately approximated using 25 terms of the infinite series.

$$\varphi_A = v_1 x + A_0 + \sum_{n=1}^{\infty} \left\{ A_n e^{k_{An} x} \cos\left(k_{An} y\right) \right\} \tag{5}$$

$$\varphi_B = v_2 x + B_0 + \sum_{n=1}^{\infty} \left\{ B_n e^{-k_{Bn} x} \cos\left(k_{Bn} y\right) \right\} \tag{6}$$

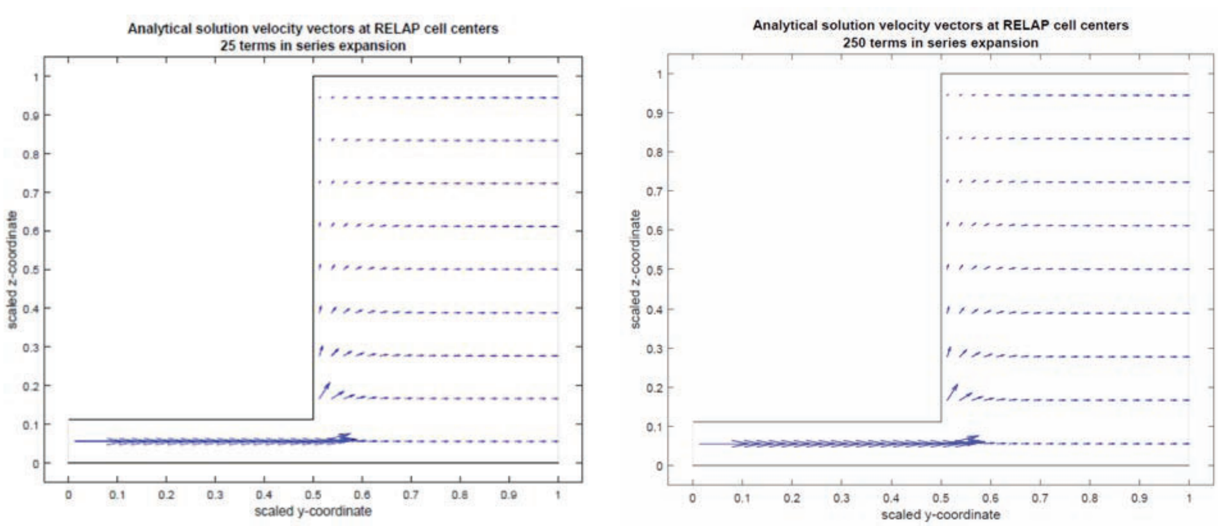

Figure 2 – Analytical solution obtained by truncating the infinite series to the first 25 terms (left) or the first 250 terms (right)

[1] The coordinate system for the solution was chosen to be consistent with the RELAP5-3D model coordinate system where x is in the depth of the page, y-axis is along the main flow direction and z-axis in the vertical direction orthogonal to the main flow direction.

4. COMPUTATIONAL MODEL RESULTS AND DISCUSSION

4.1 Backward Facing Step Model

The multi-dimensional component of RELAP5-3D is used to solve two relatively simple problems for which the analytical solution is derived from potential flow theory. The numerical model is set up assuming an incompressible, frictionless flow. Note that the multi-dimensional component has the capability of modeling the laminar viscous stress term in interior nodes (see Section 3.1.11 of [3]), however, as it will become clear in the following analysis, the numerical dissipation will mask this effect unless the flow conditions are such that momentum flux (inertia) is negligible when compared to viscous effects, or the mesh size is small enough.

The geometry for the backward facing step is based on the following:

$$a = 0.1\text{m} \quad b = 0.9\text{m} \quad L = 4.0\text{m} \tag{7}$$

The RELAP5-3D mesh for the reference model was selected to provide square mesh cells, yielding a 1x40x9 nodalization following the code coordinate system orientation. Note that the narrower inlet section (Region A) reduced to a one-dimensional mesh along the flow path.

The boundary conditions are set to be consistent with the assumptions of potential flow theory. The RELAP5-3D multi-dimensional component uses free-slip boundary conditions due to wall friction effects being lumped into the friction factor correlations within RELAP5-3D. The free slip boundary condition requires the normal velocity component at the wall to be zero and the shear stress at the wall to be zero. The free-slip boundary condition does not generate vorticity within the fluid. Therefore if the flow is specified to be irrotational at the boundaries, by setting a uniform velocity profile at the boundary, the entire flow field should be irrotational. This is because for 2D planar, inviscid, and incompressible flow, the vorticity is invariant everywhere in the flow field [5]. By turning friction off in the RELAP5-3D MULTID component, the RELAP5-3D boundary conditions are consistent with the potential flow theory assumptions. A uniform velocity of 0.1111 m/s is set at the outlet and the inlet pressure is set at 1 bar. Mass conservation leads to an inlet velocity of 1.0 m/s. The steady-state solution to the velocity field is presented in Figure 3.

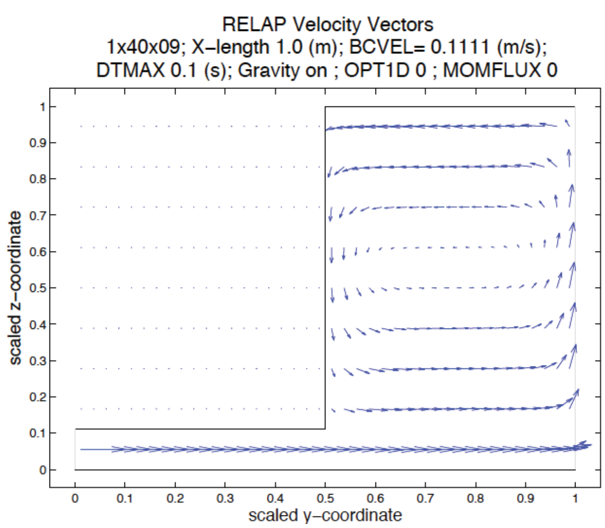

Figure 3 – RELAP5-3D predicted Flow Field

Note that the vector plot is presented in scaled coordinates therefore it is a distortion of the aspect ratio which is 40:9 in the y:z.

The solution obtained from RELAP5-3D is quite different from the potential flow solution. A large recirculation region develops in Region B. The circulation pattern in Figure 3 appears consistent to rigid-body motion with the minimum velocity located at the axis of rotation. Rigid body rotation violates irrotationality in the flow field and therefore the RELAP5-3D is not consistent with the potential flow theory requirement of irrotational flow. The uniform velocity profile at the outlet is an irrotational flow, and the RELAP5-3D multi-dimensional component free-slip boundary conditions are also consistent with potential flow theory. This leads to the question: What is responsible for the discrepancy between the RELAP5-3D solution and the potential flow solution?

RELAP5-3D solves a non-conservative form of the momentum equations, as described in Volume 1 of [3], using the phasic velocity variables v_g and v_f, as given in Eq. (2). RELAP5-3D integrates the equations considering momentum control volumes staggered relative to the control volumes for mass and internal energy. The time derivatives and convective terms are discretised with *n*-time levels on the coefficients. Moreover all derivative terms in the convective terms are donored (forward time upwind scheme – FTUS). The staggered mesh scheme used by RELAP5-3D for the multi-dimensional component is shown in Figure 4.

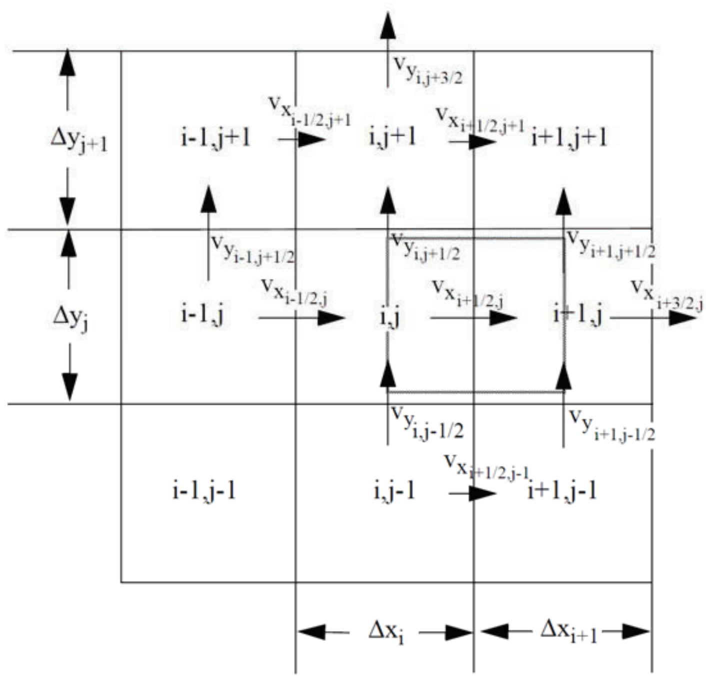

Figure 4 - Interior cells for xy plane

Following the FTUS, the discretized form of the convective term $v_x \frac{\partial v_x}{\partial x}$ results in the following:

$$v_x \frac{\partial v_x}{\partial x} \Rightarrow \begin{cases} v_{x_{i+\frac{1}{2},j}} \left(\frac{v_{x_{i+\frac{1}{2},j}} - v_{x_{i-\frac{1}{2},j}}}{\Delta x} \right) & \text{for } v_{x_{i+\frac{1}{2},j}} \geq 0 \\ v_{x_{i+\frac{1}{2},j}} \left(\frac{v_{x_{i+\frac{3}{2},j}} - v_{x_{i+\frac{1}{2},j}}}{\Delta x} \right) & \text{for } v_{x_{i+\frac{1}{2},j}} \geq 0 \end{cases} \tag{8}$$

A uniform mesh is assumed for simplicity in the notation. Consider the momentum equation for v_x and assuming $v_{x_{i+\frac{1}{2},j}} \geq 0$, the discretized form of the equation reduces to:

$$\frac{v^{n+1}_{x_{i+\frac{1}{2},j}} - v^{n}_{x_{i+\frac{1}{2},j}}}{\Delta t} + v_{x_{i+\frac{1}{2},j}} \left(\frac{v_{x_{i+\frac{1}{2},j}} - v_{x_{i-\frac{1}{2},j}}}{\Delta x} \right)^n + \overline{v}_{y_{i+\frac{1}{2},j}} \left(\frac{v_{x_{i+\frac{1}{2},j}} - v_{x_{i+\frac{1}{2},j-1}}}{\Delta y} \right)^n = \frac{P_{i,j} - P_{i+1,j}}{\Delta x} + g_x \tag{9}$$

Where $\overline{v}_{y_{i+\frac{1}{2},j}}$ is the average v_y at the point where $v_{x_{i+\frac{1}{2},j}}$ is evaluated. Now substitute the Taylor-series expansion of $v^{n+1}_{x_{i+\frac{1}{2},j}}$, $v^{n}_{x_{i-\frac{1}{2},j}}$ and $v^{n}_{x_{i+\frac{1}{2},j-1}}$, specifically:

$$\begin{aligned} v^{n+1}_{x_{i+\frac{1}{2},j}} &= v^{n}_{x_{i+\frac{1}{2},j}} + \Delta t \frac{\partial v_x}{\partial t} + \frac{1}{2}(\Delta t)^2 \frac{\partial^2 v_x}{\partial t^2} + O\left[(\Delta t)^3\right] \\ v^{n}_{x_{i-\frac{1}{2},j}} &= v^{n}_{x_{i+\frac{1}{2},j}} - \Delta x \frac{\partial v_x}{\partial x} - \frac{1}{2}(\Delta x)^2 \frac{\partial^2 v_x}{\partial x^2} - O\left[(\Delta x)^3\right] \\ v^{n}_{x_{i+\frac{1}{2},j-1}} &= v^{n}_{x_{i+\frac{1}{2},j}} - \Delta y \frac{\partial v_x}{\partial y} - \frac{1}{2}(\Delta y)^2 \frac{\partial^2 v_x}{\partial y^2} - O\left[(\Delta y)^3\right] \end{aligned} \tag{10}$$

The above expressions are substituted into Eq. (9). Then, time derivatives terms are eliminated and substituted with spatial derivatives following the manipulation suggested in Section 4.1.2 of [7] and in the appendix of [8]. After several algebraic steps the following equation can be derived:

$$\frac{\partial v_x}{\partial t} + v_x \frac{\partial v_x}{\partial x} + v_y \frac{\partial v_x}{\partial y} = \frac{v_x \Delta x}{2}(1 - c_x)\frac{\partial^2 v_x}{\partial x^2} + \frac{v_y \Delta y}{2}(1 - c_y)\frac{\partial^2 v_x}{\partial y^2} - v_x v_y \Delta t \frac{\partial^2 v_x}{\partial x \partial y} + O(3) \tag{11}$$

Where c_x and c_y are the Courant numbers in the x- and y-direction respectively:

$$\begin{aligned} c_x &= \frac{v_x \Delta t}{\Delta x} \\ c_y &= \frac{v_y \Delta t}{\Delta y} \end{aligned} \tag{12}$$

The three terms on the right hand side of Eq. (11) are a representation of the first order discretization errors as numerical or apparent diffusion, which can be expressed as artificial kinematic viscosity terms:

$$\begin{aligned} \left(\frac{\mu}{\rho}\right)_{xx,num} &= \frac{v_x \Delta x}{2}\left(1 - c_x\right) \\ \left(\frac{\mu}{\rho}\right)_{yy,num} &= \frac{v_y \Delta y}{2}\left(1 - c_y\right) \\ \left(\frac{\mu}{\rho}\right)_{xy,num} &= -v_x v_y \Delta t \end{aligned} \tag{13}$$

Note that the $\mu_{xy,num}$ can be viewed as a negative artificial compressible contribution to the viscous momentum flux introduced by the discretization errors.

Now consider that the mesh size, time step size and average velocity in the expansion assumed in the numerical solution of the problem are:

$$\begin{aligned} \Delta x &= 0.1\ m \\ \Delta t &= 0.1\ \text{s} \\ v_x &\sim 0.1\ \frac{m}{s} \end{aligned} \tag{14}$$

This results in an apparent viscosity of about 4.5 Pa-s which more than 3 orders of magnitude larger than the physical viscosity. The apparent Re number can be computed from the average x-velocity after the expansion, using the height of the channel as the characteristic length L:

$$\text{Re}_{num} = \frac{\rho U L}{\mu_{num}} = 20 \tag{15}$$

As a result, despite the codes aim to model an inviscid and incompressible flow, the truncation errors are dominating the solution such that the resulting problem is a highly viscous flow.

The dynamics of a laminar viscous flow in a channel with a sudden expansion (backward facing step) is discussed by Hawa [9]. Reference [9] derived the mathematical solution for viscous flow using the vorticity-stream function formulation and their results show the formation of a vortex behind the step. These results are also consistent with other observations [10]. These references confirm that a circulation pattern can be the result of viscous effects, which in a real problem result from the no-slip boundary condition at the wall. The inviscid flow verification problem analyzed in the present work however has apparent or numerical viscous effects that possibly induce the circulation pattern. Quantifying the impact of the numerical viscosity on the circulation is a topic for future work.

As described earlier, the numerical viscosity originates as a result of the first-order discretization of the momentum flux terms. To eliminate this effect a study was conducted by removing the momentum flux from the equation. The s flag in Word 11 of RELAP5-3D multi-dimensional component card CCC3001 controls the junction momentum flux, which can be disabled by setting *s*=3. Additionally, the 1D option for the 3D component must be enabled, which models the 3D component as having three separate 1D momentum equations. The updated solution is presented in Figure 5, which shows the solution matches reasonably well to the potential flow solution. This result is consistent with the hypothesis that the truncation error is the reason behind the RELAP5-3D solution shown in Figure 3.

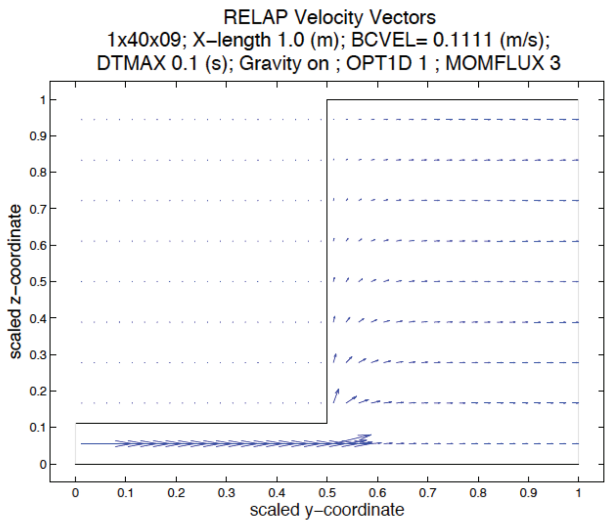

Figure 5 - RELAP5-3D predicted Flow Field with momentum flux terms disabled

4.2 2D Vessel with Downcomer Model

Similar discretization effects are analyzed with another problem for which the potential flow theory solution has been presented by Yeh [6]. The problem is a simplified 2D representation of the flow from the downcomer to the reactor core in a representative PWR. The figure from the 1975 paper from Yeh is reproduced below (shown with the symmetry plane on the right boundary). The geometry here is a 2D rectangular domain, with the total height of 3.0 m, and the bottom of the downcomer (core barrel) located at 1.0 m from the bottom of the vessel. The vessel width is assumed to be 4.0 m.

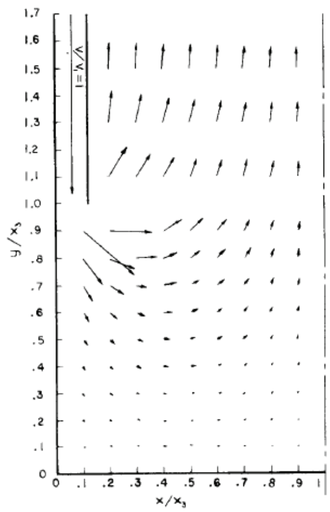

Fig. 3. Velocity distribution in a two-dimensional lower plenum. The parameters are: $x_1/x_3 = x_2/x_3 = 0.117$, $y_1/x_3 = 1$, and $L/x_3 = 3$. The velocity is normalized with the inlet velocity V_1.

Figure 6 – Figure 3 from Yeh (1975) [6]

The RELAP-3D solution is obtained following the same method presented for the backward facing step problem. First the solution is obtained assuming the default formulation of the momentum equations. Then the momentum flux terms are disabled. Both solutions are presented in Figure 7 with the default formulation shown on the left and the solution with disabled momentum flux terms on the right. As seen with the backward facing step problem, the potential flow solution can only be reasonably approximated well when the momentum flux terms are removed. The default solution shows a significant internal circulation pattern, which should not occur for an inviscid, irrotational flow. A possible explanation is that the first-order discretization of the momentum flux terms changes the nature of the flow to be artificially viscous flow.

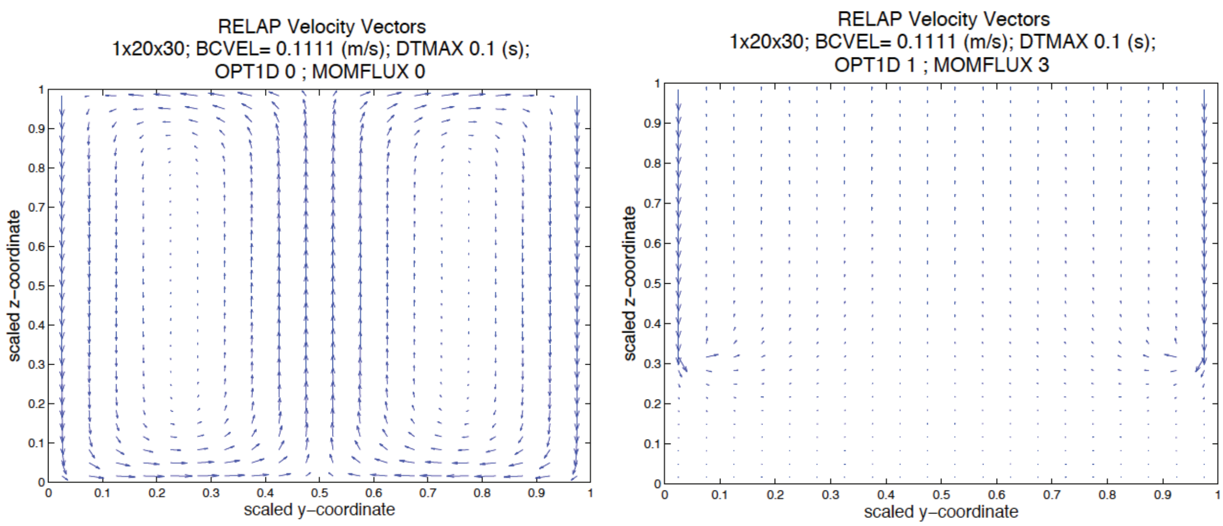

Figure 7 – RELAP5-3D solution of the simplified downcomer-lower-plenum-core of a reference PWR with (on the left) and without (on the right) momentum fluxes considered in the solution

5. CONCLUSIONS

The fundamental studies presented in this paper are intended to investigate possible limitations and shortcomings in modeling multidimensional flow with the thermal-hydraulic system code RELAP5-3D. The user should be aware of these limitations when multi-dimensional flow features and phenomena are determined to be important for the specific application and goals of the system analysis.

The question addressed here is the adequacy of the RELAP5-3D 3D formulation to simulate single-phase incompressible flow within the context of geometries and nodalizations typically considered in RELAP5-3D applications. Following a bottom-up analysis, the most simple multidimensional flow solution is for the incompressible, frictionless flow.

Numerical predictions from RELAP5-3D were benchmarked to analytical solutions from potential flow theory derived for relatively simple geometries. The study shows a strong distortion potentially associated with the first-order discretization of the advection term. The potential flow solution is better approximated when momentum flux terms are not modeled. However this would introduce an error in the pressure field solution when momentum flux terms are important.

The user needs to be particularly aware of the effects of numerical viscosity when considering modeling viscous laminar flow with the code. Artificial viscosity due to discretization errors could mask any physical effect of the viscosity unless precautions are taken in the choice of mesh and time step size.

6. REFERENCES

[1] C. Frepoli, J. Fricano, J. Yurko, F. Buschman and D. Aumiller, "On the Defintion of a Minimum Set of Requirements to Assess the Adequacy of the RELAP5-3D Multidimensional Flow Capability with Selected Canonical Problems," in *NURETH-16, Log Number 13213*, 2015.

[2] C. Frepoli, J. Fricano, F. Buschman and D. Aumiller, "Simulation of Faraday Waves with RELAP5-3D Thermal-Hydraulic Codes," in *The 16th International Topical Meeting on Nuclear Reactor Thermal Hydraulics (NURETH-16)*, 2015.

[3] T. R.-3. C. D. Team, "RELAP5-3D© Code Manual Volume I: Code Structure, System Models and Solution Methods," Idaho Falls, Idaho, 1999.

[4] P. S. Damerell and J. W. Simons, "Reactor Safety Issues Resolved by the 2D/3D Program," U.S. NRC, Washington, DC, 1993.

[5] E. Greitzer, C. Tan and M. Graf, Internal Flow: Concepts and Applications, New York: Cambridge University Press, 2004.

[6] H. Yeh, "METHOD OF SOLVING THE POTENTIAL FIELD IN COMPLICATED GEOMETRIES AND THE POTENTIAL FLOW IN THE LOWER PLENUM OF A PRESSURIZED WATER REACTOR," no. 32 85-104, 1975.

[7] J. Tannehill, D. Anderson and R. Pletcher, Computational Fluid Mechnics and Heat Transfer, Second Edition, Taylor&Francis, 1997.

[8] K. Ohkawa and C. Frepoli, "Simulation of Farday Waves in Downcomer Geometry of PWR with WCOBRA/TRAC," Tokyo, Japan, 2003.

[9] T. Hawa and Z. Rusak, "The dynamics of a laminar flow in a symmetric channel with a sudden expansion," Vols. vol. 436, pp. 283–320, no. J. Fluid Mech., 2001.

[10] F. Battaglia and e. al., "Bifurcation of Low Reynolds Number Flows in Symmetric Channels," vol. Vol. 35 No. 1, no. AIAA Journal, 1997.

[11] G. Biswas, M. Breuer and F. Durst, “Backward-Facing Step Flows for Various Expansion Ratios at Low and Moderate Reynolds Numbers,” vol. 126, no. Journal of Fluids Engineering, 2004.

APPENDIX A

The problem is divided into two regions. Region A is the narrower inlet section and region B is after the expansion. Within each region, the solutions are obtained with the method of separation of variables by solving the Laplacian in two dimensions:

$$\frac{\partial^2 \varphi}{\partial x^2} + \frac{\partial^2 \varphi}{\partial y^2} = 0 \tag{16}$$

With the following inflow and outflow boundary conditions (B.C.):

$$\begin{aligned} \frac{\partial \varphi_A}{\partial x} &= v_1,\ x = -\infty; \\ \frac{\partial \varphi_B}{\partial x} &= v_2,\ x = +\infty; \end{aligned} \tag{17}$$

The y-component of the velocity is zero at the symmetry plane and at the upper horizontal wall boundaries:

$$\begin{aligned} \frac{\partial \varphi_A}{\partial y} &= 0,\ \mathrm{y} = 0,\ \mathrm{y} = a; \\ \frac{\partial \varphi_B}{\partial y} &= 0,\ \mathrm{y} = 0,\ \mathrm{y} = b; \end{aligned} \tag{18}$$

The x-component of the velocity is zero at the vertical wall within Region B:

$$\frac{\partial \varphi_B}{\partial x} = 0,\ a \le \mathrm{y} \le b \tag{19}$$

The form of the solution in each region is represented by infinite series as follows:

$$\varphi_A = v_1 x + A_0 + \sum_{n=1}^{\infty} \left\{ A_n e^{k_{An} x} \cos\left(k_{An} y\right) \right\} \tag{20}$$

$$\varphi_B = v_2 x + B_0 + \sum_{n=1}^{\infty} \left\{ B_n e^{-k_{Bn} x} \cos\left(k_{Bn} y\right) \right\} \tag{21}$$

Where it can be shown that the velocities v_1 and v_2 satisfy the continuity equation over the entire domain:

$$v_2 = \frac{a}{b} v_1 \tag{22}$$

The coefficients in Equations (20) and (21) are obtained solving the following set of equations:

$$A_0 = B_0 + \frac{1}{a} \sum_{n=1}^{\infty} \left\{ B_n \int_0^a \cos\left(k_{Bn} y\right) dy \right\} \tag{23}$$

$$A_m = \frac{2}{a} \sum_{n=1}^{\infty} \left\{ B_n \int_0^a \cos\left(k_{Bn} y\right) \cos\left(k_{Am} y\right) dy \right\}; \quad \text{for } m = 1, 2, \ldots \tag{24}$$

After significant manipulation of Eq. (23) and Eq. (24) the relationship among the coefficients is obtained as:

$$-\frac{k_{Bj} B_j b}{2} - \sum_{m=1}^{\infty} \left\{ k_{Am} \left[\frac{2}{a} \sum_{n=1}^{\infty} \left\{ B_n I\left(k_{Am}, k_{Bn}\right) \right\} \right] I\left(k_{Am}, k_{Bj}\right) \right\} = \frac{v_1}{k_{Bj}} \sin\left(\frac{j\pi a}{b} \right)$$

Where

$$I\left(k_{Am}, k_{Bn}\right) = \int_0^a \cos\left(k_{Bn} y\right) \cos\left(k_{Am} y\right) dy \tag{25}$$

$$I\left(k_{Am}, k_{Bj}\right) = \int_0^a \cos\left(k_{Bj} y\right) \cos\left(k_{Am} y\right) dy$$

Note that at a particular *m*, $I\left(k_{Am}, k_{Bj}\right)$ is a constant, so it can be put within the *n*-series summation:

$$-\frac{k_{Bj} B_j b}{2} - \sum_{m=1}^{\infty} \left\{ k_{Am} \frac{2}{a} \sum_{n=1}^{\infty} \left\{ B_n I\left(k_{Am}, k_{Bn}\right) I\left(k_{Am}, k_{Bj}\right) \right\} \right\} = \frac{v_1}{k_{Bj}} \sin\left(\frac{j\pi a}{b} \right) \tag{26}$$